Homogeneous Catalysis

How to cite:
International Edition: doi.org/10.1002/anie.202115983
German Edition: doi.org/10.1002/ange.202115983

Proton-Promoted Nickel-Catalyzed Asymmetric Hydrogenation of Aliphatic Ketoacids

Chen-Qiang Deng, Jiao Liu, Jia-Hao Luo, Li-Jin Gan, Jin Deng, and Yao Fu**

Abstract: *A robust and highly active homogeneous chiral nickel–phosphine complex for the asymmetric hydrogenation of aliphatic γ- and δ-ketoacids has been discovered. The hydrogenation could proceed smoothly in the presence of 0.0133 mol% catalyst loading (S/C = 7500). The coordination chemistry and catalytic behavior of $Ni(OTf)_2$ with (S,S)-Ph-BPE were explored by ^1H NMR and HRMS. The mechanistic studies revealed that a proton promoted the activation of the substrate C=O bond and controlled the stereoselectivity through hydrogen bonds. A series of chiral γ- and δ-alkyl substituted lactones were obtained in high yields with excellent enantioselectivities (up to 98% yield and 99% ee). In addition, this catalytic system also demonstrated that levulinic acid produced from a biomass feedstock was converted into chiral γ-valerolactone without loss of ee value.*

Introduction

The catalytic conversion of renewable resources into valuable chemicals has aroused widespread interest recently in academia and industry. Biomass, as a renewable and sustainable organic carbon resource, is regarded as the most promising substitute for petroleum derivatives.[1] Levulinic acid (LA), as an important biomass-derived platform molecule, can be transformed into other high value-added chemicals such as diols,[2] carboxylic acids,[3] and lactone.[2c, 4] Compared to achiral lactones, chiral lactones are versatile building blocks to construct many important natural products and biologically active molecules.[5] In addition, it is also widespread in nature, in particular pheromones and aromatic components of many fruits.[6] Some methodologies have been reported for the synthesis of chiral lactones to date, including asymmetric hydrogenation,[7] hydroboration,[8] and biocatalysis.[9] Among them, asymmetric hydrogenation is undoubtedly a powerful and effective approach for the manufacture of chiral molecules.[10] In the past few decades, the catalytic asymmetric hydrogenation of ketone has made great achievements in precious metal catalysts based on ruthenium, rhodium, and iridium as an active center,[11] exhibiting excellent catalytic activity and enantioselectivity (Scheme 1). In 2015, the Mika group reported the SegPhos-Ru-catalyzed asymmetric reduction of biomass-derived levulinic acid to γ-valerolactone (GVL) in 64% yield with 82% ee under 60 atm H_2 at 140 °C.[7a] More recently, Zhou and co-workers described iridium complexes with a chiral P–N ligand to catalyze the asymmetric hydrogenation of levulinic acid with high enantioselectivity.[7b] However, due to decreasing reserves, high prices, and toxicity of these precious metals, it is very necessary to replace them with earth-abundant, inexpensive, and environmentally benign metals.

The earth-abundant first-row transition metals have attracted intensive attention in homogeneous asymmetric hydrogenation of ketone in recent years.[12,13] In 2014, Morris and co-workers reported for the first time cheap iron pincer complexes with chiral tridentate PNP ligands for the asymmetric hydrogenation of ketones.[14] In this catalyst system, aromatic ketones could be hydrogenated with up to 85% ee, but aliphatic ketone substrates afforded a racemic product. After this, all sorts of chiral iron pincer complexes are also developed for the asymmetric hydrogenation of C=O bonds.[15] In addition to these cheap iron catalysts, chiral manganese complexes in ketone reduction have been reported successively. Clarke and Beller in 2017 described manganese complexes with chiral tridentate ligands for the

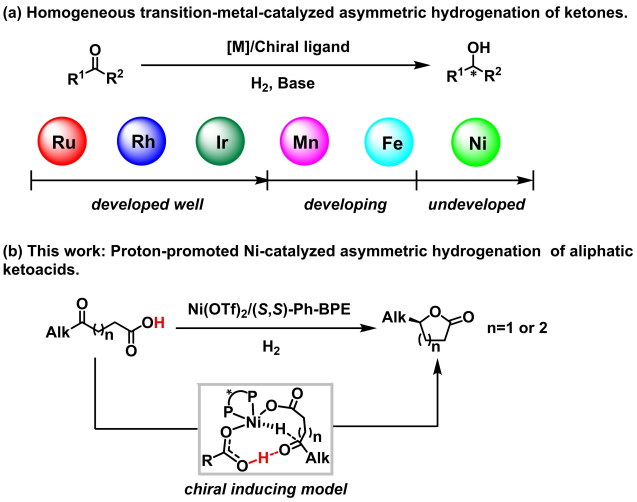

Scheme 1. The asymmetric hydrogenation of C=O bonds.

[*] C.-Q. Deng, J. Liu, J.-H. Luo, L.-J. Gan, Prof. Dr. J. Deng, Prof. Dr. Y. Fu
Hefei National Laboratory for Physical Sciences at the Microscale, iChEM, CAS Key Laboratory of Urban Pollutant Conversion, Anhui Province Key Laboratory of Biomass Clean Energy, Department of Applied Chemistry, University of Science and Technology of China, Hefei, Anhui 230026 (China)
E-mail: dengjin@ustc.edu.cn
fuyao@ustc.edu.cn

hydrogenation of simple ketones, respectively;[13a,b] however, the reaction gave lower enantiomeric ratios for most ketone substrates. Recently, Ding and co-workers demonstrated that aromatic ketones were hydrogenated with high ee values using chiral pincer PNN–Mn catalysts.[13c] Notably, all these reported cheap catalysts prefer to hydrogenate aromatic ketone with high enantioselectivity, while dialkyl ketone generally gives a lower enantiomeric ratio. Besides, these catalyst systems require extra bases as additives to activate the precatalyst. Hence, it is still a high challenge to develop earth-abundant first-row transition metal catalysts for the asymmetric hydrogenation of dialkyl ketone with high enantiomeric excess.

Among these first-row transition metals, nickel elements have fascinated increasing attention in asymmetric reduction.[10d, 16] In 2016, Chirik and co-workers developed the first example of nickel-catalyzed asymmetric hydrogenation of α,β-unsaturated esters.[10d] Subsequently, Zhang and co-workers reported a chain of studies on the nickel-catalyzed asymmetric hydrogenation of functionalized enamides and cyclic sulfamidate imines with excellent results.[16a–d] Recently, Zhang and co-workers disclosed the asymmetric hydrogenation of N-sulfonyl imines, N-aryl imino esters, and 2-amidoacrylates using nickel catalysts and molecular hydrogen as reducing agents, affording a series of chiral amines and amino acids with high enantiomeric excesses.[16e–h] These examples demonstrate that catalysts containing earth-abundant first-row transition metal have great potential in the asymmetric hydrogenation of prochiral molecules. Despite nickel-catalyzed asymmetric reduction having seen rapid growth, the asymmetric hydrogenation of ketones is still in the beginning stage. To the best of our knowledge, so far, only two examples of nickel-catalyzed asymmetric hydrogenation of ketones have been reported by Hamada and co-workers.[17] In the two cases, α-amino-β-ketoesters hydrochlorides and substituted aromatic α-amino ketones hydrochlorides were hydrogenated to afford the corresponding products via dynamic kinetic resolution using $Ni(OAc)_2$/(*R*,*S*)-ferrocenyl ligand at 100 atm H_2; however, it was not suitable for aliphatic ketoester substrates. Furthermore, the mechanism of hydrogen activation and chiral inducing mode has not yet been elucidated. Given this limited precedent, it is not surprising that there are still no examples of the asymmetric hydrogenation of dialkyl ketones using homogeneous chiral nickel catalysts. Herein, we report for the first time the nickel-catalyzed asymmetric hydrogenation of aliphatic γ- and δ-ketoacids to afford chiral lactones with high yields and excellent enantioselectivities.

Results and Discussion

Initially, we performed various chiral biphosphine ligands in combination with nickel triflate for the asymmetric hydrogenation of levulinic acid under 1 atm H_2 at 50 °C for 12 hours. These results are shown in Scheme 2. When axially chiral ligands were employed, the hydrogenation afforded lower enantioselectivities (14–37 % ee). The (*S*,*S*)-DuPhos produced only a trace amount of GVL. By electron-rich

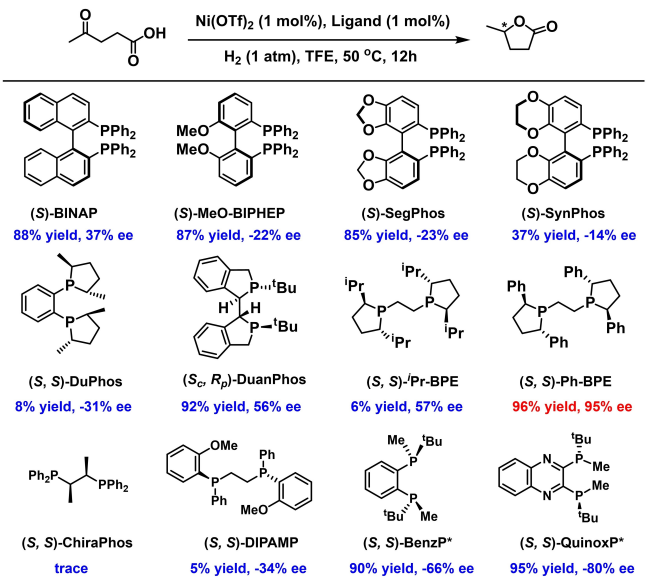

Scheme 2. Ligand screening for the asymmetric hydrogenation of LA. Reaction conditions: 1 mmol levulinic acid, 1 mol% $Ni(OTf)_2$, 1 mol% Ligand, 2 mL TFE, 1 atm H_2, 50 °C, and 12 hours. The ee values were determined by GC analysis on a chiral stationary phase. TFE: 2,2,2-trifluoroethanol.

(*S*,*S*)-DuanPhos instead of (*S*,*S*)-DuPhos, the GVL yield and enantioselectivity increased to 92 % and 56 %, respectively. The (*S*,*S*)-^{i}Pr-BPE resulted in very poor reactivity. To our delight, using phenyl to replace the isopropyl group in BPE ligand, (*S*,*S*)-Ph-BPE could dramatically improve the catalytic activity, and full conversion with excellent enantioselectivity was achieved (96 % yield, 95 % ee). Furthermore, (*S*,*S*)-BenzP* and (*S*,*S*)-QuinoxP* furnished high GVL yields and moderate and good enantioselectivities. To better understand the difference in reactivity between the phenyl and isopropyl substituents of BPE ligand, we analyzed the binding pocket steric of $[(S,S)\text{-}^i\text{Pr-BPE})Ni]^{2+}$ and [(*S*,*S*)-Ph-BPE)Ni]$^{2+}$ complex using the SambVca 2.1 Web program (Figure 1).[18] According to the buried volumes ($\%V_{bur}$), complex **2** ($\%V_{Bur}=80.3$) possessed a more congested catalytic pocket than complex **1** ($\%V_{Bur}=65.5$). The enhanced steric congestion at the binding pocket of complex **2** correlated with its excellent catalytic performance. The steric maps illustrated that complex **1** and **2** presented the expected space occupation of less hindered NE and SW quadrants than NW and SE quadrants, indicating that two complexes should be given the same configuration product.

Next, we screened the effect of nickel salts on hydrogenation. The results of various nickel salts were listed in Table 1. When $Ni(OTf)_2$ and $Ni(BF_4)_2{\cdot}6H_2O$ were used, the reactions furnished high GVL yield with excellent enantioselectivity (entries 1 and 2). With the use of $Ni(OAc)_2$ and $Ni(OAc)_2{\cdot}4H_2O$ as the nickel precursor, the catalytic activity decreased slightly but ee values remained constant (entries 3 and 4). However, the reactions took place poorly or even failed by using $NiCl_2$ and Ni(acac)$_2$ (entries 5 and 6). These results showed that the nickel precursor plays an important

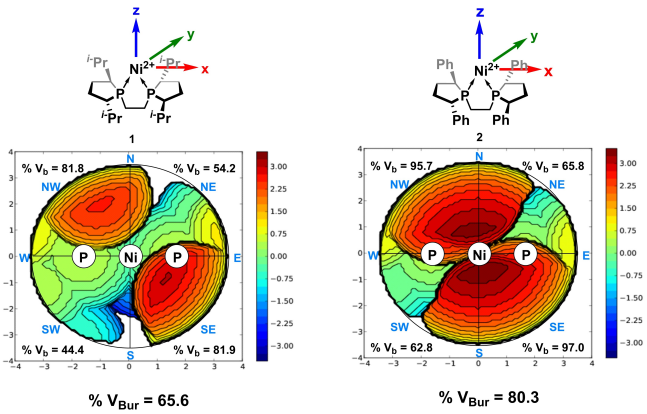

Figure 1. The steric maps of nickel complexes with biphosphine ligands. NE: northeast; SE: southeast; SW: southwest; NW: northwest.

Table 1: Nickel sources screening for the asymmetric hydrogenation of LA.[a]

Entry	Nickel sources	Yield [%]	ee [%]
1	$Ni(OTf)_2$	96	95
2	$Ni(BF_4)_2{\cdot}6H_2O$	96	95
3	$Ni(OAc)_2$	75	95
4	$Ni(OAc)_2{\cdot}4H_2O$	77	96
5	$NiCl_2$	5	94
6	$Ni(acac)_2$	0	-

[a] Reaction conditions: 1 mmol levulinic acid, 1 mol% nickel sources, 1 mol% (*S*,*S*)-Ph-BPE, 2 mL TFE, 1 atm H_2, 50 °C, and 12 hours.

role in catalytic efficiency. To further improve the enantiocontrol, the hydrogenation solvents were also evaluated (see the Supporting Information). It turned out that TFE gave the best results for this reaction, while other solvents afforded GVL in low yields with moderate enantioselectivities. On the one hand, TFE has good solubility for ketoacids, and on the other hand, it bears suitable acidity and weak coordination ability, which may be the reason for its excellent results.

The effect of the molar ratio of $Ni(OTf)_2$ with (*S*,*S*)-Ph-BPE on reactivity was investigated, as listed in Table 2. It was found that an excessive amount of (*S*,*S*)-Ph-BPE ligand resulted in low reactivity (entry 1). However, increasing the amount of nickel triflate had no effect on hydrogenation activity (entry 3). It was speculated that it may be due to the difference in coordination mode of nickel triflate with the ligand, which leads to the decrease of reactivity. To prove this conjecture, the coordination mode of $Ni(OTf)_2$ with (*S*,*S*)-Ph-BPE was explored by ^1H NMR and HRMS (see the Supporting Information). The results of ^1H NMR indicated that the mixture signals markedly changed compared with (*S*,*S*)-Ph-BPE. According to the ESI-MS spectrum of the $Ni(OTf)_2$/(*S*,*S*)-Ph-BPE = 1/1 mixture, a mono-ligand coordinated nickel complex ($[(S,S)\text{-Ph-BPE})Ni]^{2+}$, *m*/*z* 282.0861) was detected, with none of other the form of nickel complex being found. However, a dual-ligand coordinated nickel complex ($[(S,S)\text{-Ph-BPE})_2Ni]^{2+}$, *m*/*z* 535.1973) was observed in the $Ni(OTf)_2$/(*S*,*S*)-Ph-BPE = 0.25/1 mixture. It demonstrated that the mono-ligand coordinated nickel complexes act as active species in the hydrogenation, rather than that of dual-ligand coordinated nickel complexes. In addition, the results of the ESI-MS spectrum showed that all of the complexes existed in the form of cation, while anionic and neutral complexes were not observed. It was worth mentioning that inactive $[(S,S)\text{-Ph-BPE})_2Ni]^{2+}$ could be dissociated by adding nickel triflate to form active $[(S,S)\text{-Ph-BPE})Ni]^{2+}$ (Scheme 3).

To evaluate the efficiency of this catalytic system, the hydrogenation was examined in the presence of low catalyst loading (see the Supporting Information, Table S2). With the use of 0.1 mol% catalyst loading, levulinic acid was hydrogenated to obtain GVL in 98 % yield with 95 % ee at 30 atm H_2 for 4 hours. When the catalyst loading was further reduced to 0.0133 mol% (S/C = 7500), the hydrogenation could be also smoothly proceeded at 70 atm H_2 for 24 hours, affording GVL in 94 % yield with 95 % ee. Compared with precious metal catalysts,[7] the chiral nickel catalyst demonstrated excellent reactivity and enantioselectivity in asymmetric hydrogenation of aliphatic ketoacids. So far, this result represents the highest catalytic efficiency of the reported nickel-catalyzed asymmetric hydrogenation of C=O bonds.

In order to further understand the reaction pathway, ethyl levulinate and angelica lactone as the substrate were used for hydrogenation, respectively. When angelica lactone was used as the substrate, the hydrogenation could be not proceeded under standard reaction conditions (Scheme 4a). However, with the use of ethyl levulinate as the substrate, GVL could be obtained in 85 % yield with 78 % ee (Scheme 4b). It demonstrated that the carbonyl group of the substrate was first hydrogenated to generate 4-hydroxyvaleric acid and followed by cyclization to obtain GVL. Then adding one equivalent acetic acid into the reaction system, the yield and enantioselectivity of GVL improved to 94 % and 91 % ee, respectively (Scheme 4c). However, when sodium levulinate was employed as the substrate, the hydrogenation gave similar results to ethyl levulinate (Scheme 4d). These results indicated that protons play an important role in activating the C=O bond and controlling stereoselectivity.

Table 2: The effect of the molar ratio of $Ni(OTf)_2$ with (*S*,*S*)-Ph-BPE.

Entry	M/L	Yield [%]	ee [%]
1	1/4	64	95
2	1/1	96	95
3	4/1	96	95

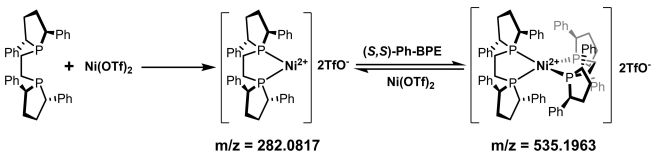

Scheme 3. The coordination mode of $Ni(OTf)_2$ with (*S*,*S*)-Ph-BPE.

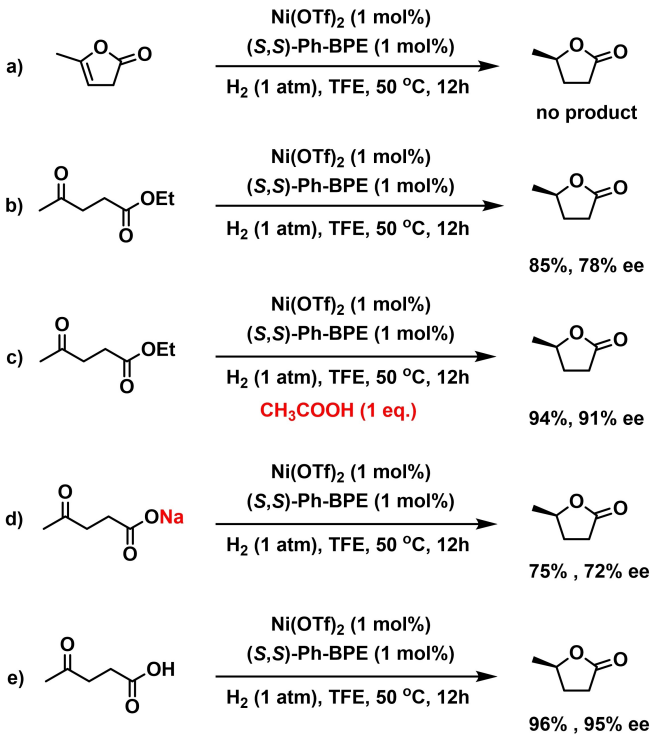

Scheme 4. The control experiments.

Subsequently, we performed several deuterium labeling experiments. In the presence of H_2, deuterium incorporation at the γ-carbon position in 8% ratio was observed by replacing CF_3CH_2OH with CF_3CH_2OD (Scheme 5a). It was probably because the combination of the Ni–H species with CF_3CH_2OD or deuterated levulinic acid (from levulinic acid and CF_3CH_2OD exchange) generated HD, and subsequent the heterolytic cleavage H–D bond formed the Ni–D species to attack C=O bonds, resulting in deuterium being incorporated into the γ-carbon position. This result further proved that TFE had suitable acidity and proton donating ability. Next, the hydrogenation using D_2 furnished 84% D of the product in CF_3CH_2OH (Scheme 5b). It was found that deuterium incorporation was only observed at the γ-carbon position, further confirming that the reaction process of levulinic acid had not undergone angelica lactone and enolization to hydrogenate C=C bonds. In the presence of D_2, a 97% D of the product was obtained in CF_3CH_2OD (Scheme 5c). Furthermore, the hydrogenation afforded a 100% D of the product by using deuterated levulinic acid as the substrate under the above reaction conditions (Scheme 5d). These results indicated that the combination of protons with metal hydrides and the heterolysis of hydrogen gas were in equilibrium.

To better gain insight into the mechanism of this reaction, we performed DFT calculations for this Ni-catalyzed asymmetric hydrogenation of levulinic acid with the Ni(L=(*S*,*S*)-Ph-BPE)-H complexes as the energy reference point (Figure 2). From **Int1**, there were two possible pathways for the hydrogenation of LA: the *R* pathway and the *S* pathway. The calculated energy of the transition state **R-TS1** was 3.7 kcal mol^{-1} lower than that of the transition state **S-TS1**, indicating that the hydrogenation should give the *R* configuration product with excellent enantioselectivity, which was consistent with the experimental result (95% ee). The energy difference between two transition states may be attributed to the orientation of the Ni–H formation in the presence of LA. In addition, the transition state suggested that the proton could activate the C=O bond and anchor it through hydrogen bonds to control stereoselectivity. Based on the mechanistic experiments and literature reports,[10d, 16c,g] we proposed the following reaction mechanism in Scheme 6. A square-planar complex species **A** was generated in the presence of LA. Then heterolytic H–H bond formed metal hydride species **B** and released a

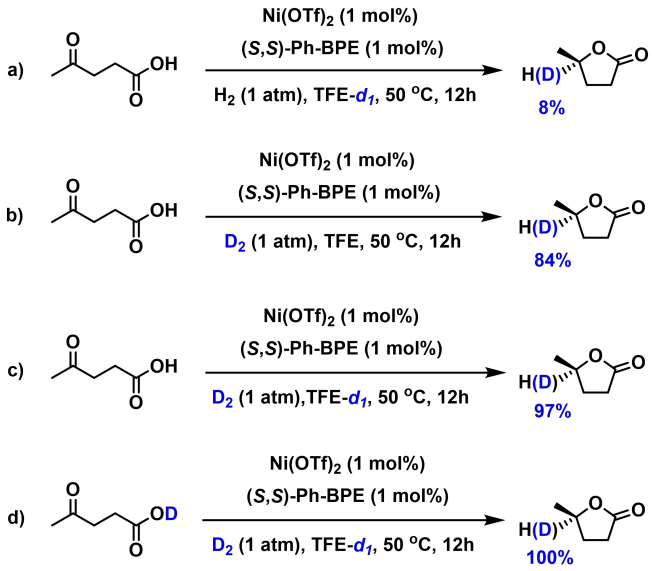

Scheme 5. The deuterium-labelling experiments.

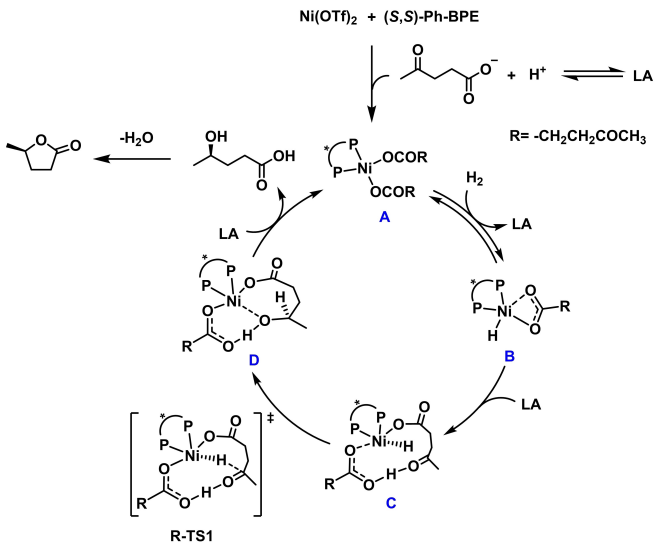

Scheme 6. A proposed reaction mechanism.

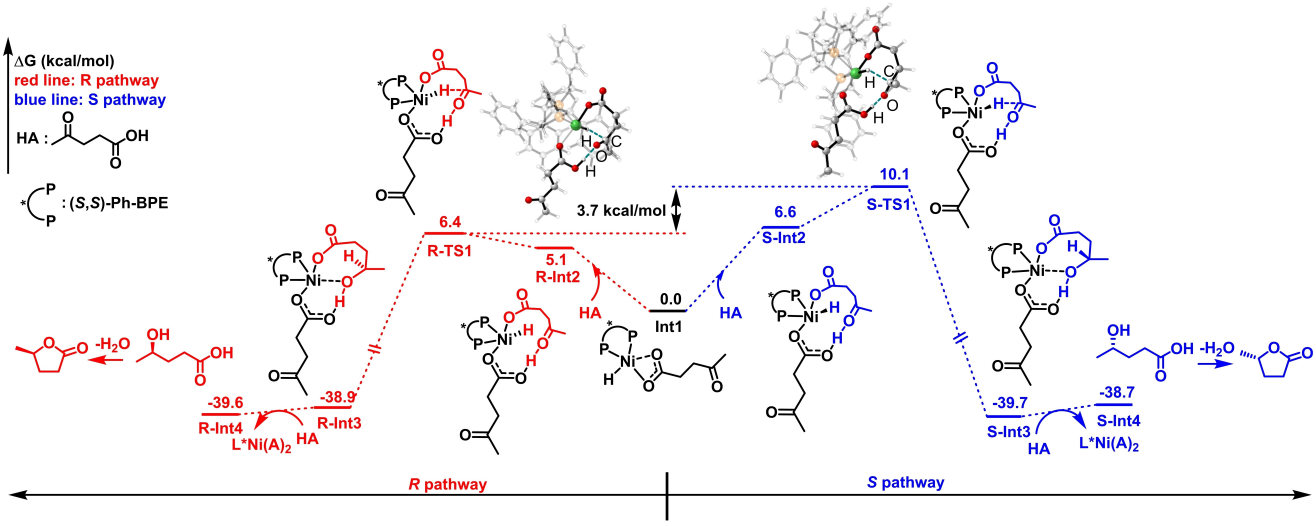

Figure 2. Calculated Gibbs free energy profile for the configuration-determining step (kcal mol^{-1}). Int: intermediate, TS: transition state, HA: levulinic acid.

molecule of LA, and subsequent LA coordinated with the nickel(II) metal center to produce species **C**. Next, the Ni–H attacked C=O bonds to yield species **D**. It would react with LA to obtain 4-hydroxyvaleric acid and regenerate species **A**. Finally, (*R*)-GVL was obtained by intramolecular esterification.

To establish the general applicability of this chiral nickel catalyst, the hydrogenation of different aliphatic ketoacids was investigated. These results were shown in Scheme 7. The linear aliphatic γ-ketoacid substrates could provide the corresponding products **2a**–**2e** in 91 %-98 % yields with 95–97 % ee. The reactions of the substrate bearing branched alkyl and cycloalkyl group were smoothly proceeded to afford the products **2f**–**2j** with 96–99 % ee. It was worth mentioning that the hydrogenation could be also successfully performed on the large sterically hindered substrate (R = ^{t}Bu, **1h**). Two methyl groups were introduced at the α- and β- positions of the substrate to obtain products **2k** and **2l** with 92 % ee and 96 % ee, respectively. Interestingly, the C=C bond of the substrate **1m** was tolerated. The substrates containing the benzyl and carboxyl group resulted in moderate enantioselectivities (**2n** and **2o**). More importantly, aliphatic δ-ketoacid substrates were also applicable. The substrates with linear alkyl group **1p**–**1r** gave the desired products in 91–95 % yield with 84–91 % ee. The long-chain alkyl δ-ketoacids slightly decreased ee values. A dimethyl group at β-position substrate afforded the product **2s** in 96 % yield with 96 % ee. Compared to the biocatalytic method,[9] these results suggested that this cheap nickel catalyst system has broader applicability to ketoacid substrates.

The synthesis of the chiral GVL from real biomass-derived levulinic acid was essential to demonstrate the compatibility of this catalytic system. First, D-fructose was hydrolyzed in 0.5 M H_2SO_4 at 170 °C for 1 hour. Then the solution was extracted with ethyl acetate and removed in a vacuum to afford levulinic acid as a dark brown viscous liquid.[19] Considering the influence of humins or other oxygenated compounds on nickel triflate, the reaction was conducted using excessive nickel salt (Scheme 8A). As a result, GVL could be obtained in 94 % yield with 95 % ee. Next, we exhibited that levulinic acid from biomass feedstock transformed into (*R*)-GVL (Scheme 8B). The bamboo powder was hydrolyzed in 1.0 M H_2SO_4 at 170 °C for 8 hours; a deep dark brown solution was obtained.[19a] Levulinic acid then was obtained by vacuum distillation for subsequent reaction. The hydrogenation furnished (*R*)-GVL in 97 % yield with 95 % ee in presence of 0.1 % mol $Ni(OTf)_2$/(*S*,*S*)-Ph-BPE. Undoubtedly, chiral GVL with a high enantiomeric ratio could be produced from real biomass-derived levulinic acid. This study provides an excellent protocol for the preparation of high value-added fine chemicals from biomass raw materials.

In order to demonstrate the scale-up potential of this protocol, the hydrogenation was conducted on a larger scale at 0.02 mol% catalyst loading (Scheme 9a). 11.6 g levulinic acid was completely transformed into (*R*)-GVL in 91.2 % isolated yield with 96 % ee using (*S*,*S*)-Ph-BPE under 70 atm H_2 at 50 °C for 12 hours. Likewise, (*S*)-GVL could be also obtained by using (*R*,*R*)-Ph-BPE. The scale-up reaction still maintained high reactivity and excellent enantioselectivity. Next, the utility of this methodology was demonstrated by further conversion of chiral GVL (Scheme 9b and c). The chiral GVL could be easily converted to ***(R)*-4** and ***(S)*-6**,[20,5b] which are precursors of the P-Chirogenic PhosPholane ligand and natural product (*S*)-(+)-phoracantholide I, respectively.

Conclusion

In summary, we have developed a robust and efficient chiral nickel–phosphine complex for the asymmetric hydrogenation of aliphatic ketoacids. The hydrogenation could proceed on a ten gram-scale in the presence of 0.02 mol% catalyst loading. The control experiments, deuterium-labeling experiments, and DFT calculations have provided

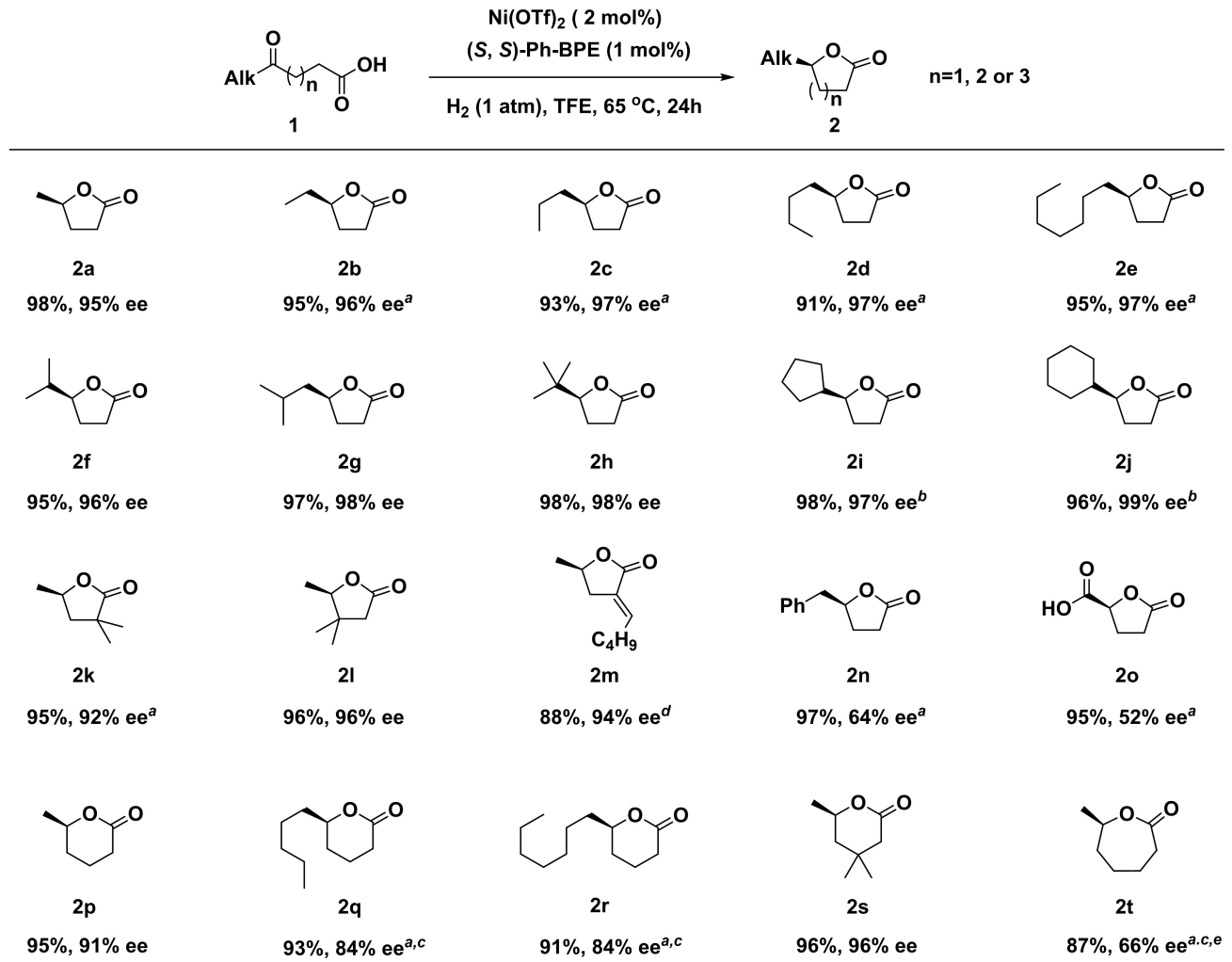

Scheme 7. The substrate scope of asymmetric hydrogenation. Reaction conditions: 0.25 mmol substrates, 2 mol% $Ni(OTf)_2$, 1 mol% (*S*,*S*)-Ph-BPE, 1 atm H_2, 2 mL TFE, 65 °C, and 24 h. The yield was determined by GC analysis. The ee values of the products were determined by GC analysis on a chiral stationary phase. [a] 50 atm H_2. [b] 10 atm H_2. [c] 5 mol% $Ni(OAc)_2 \cdot 4H_2O$/(*S*,*S*)-Ph-BPE and 50 °C. [d] 2 mL DCM, 30 atm H_2, and 50 °C. [e] Followed by Yamaguchi cyclization.

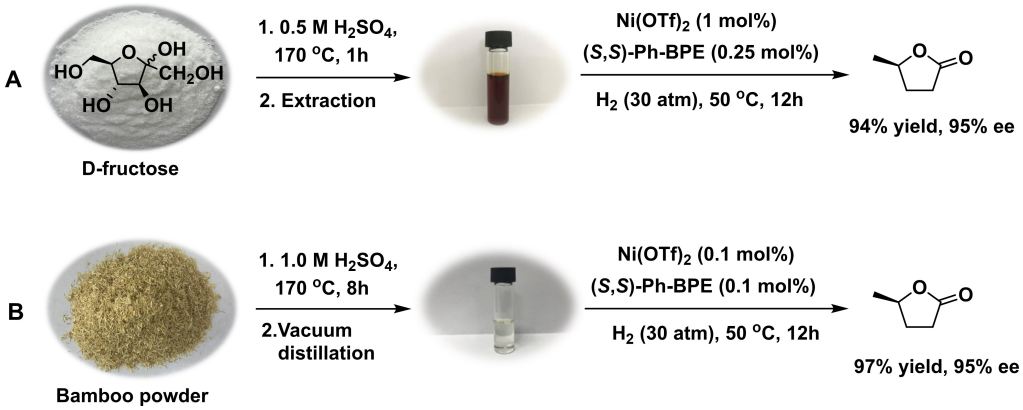

Scheme 8. The conversion of D-fructose and bamboo powder into (*R*)-GVL.

mechanistic understanding for this Ni-catalyzed asymmetric hydrogenation of levulinic acid, confirming a proton plays a key role in the activation of the C=O bond and the stereoselectivity control. The general applicability of this

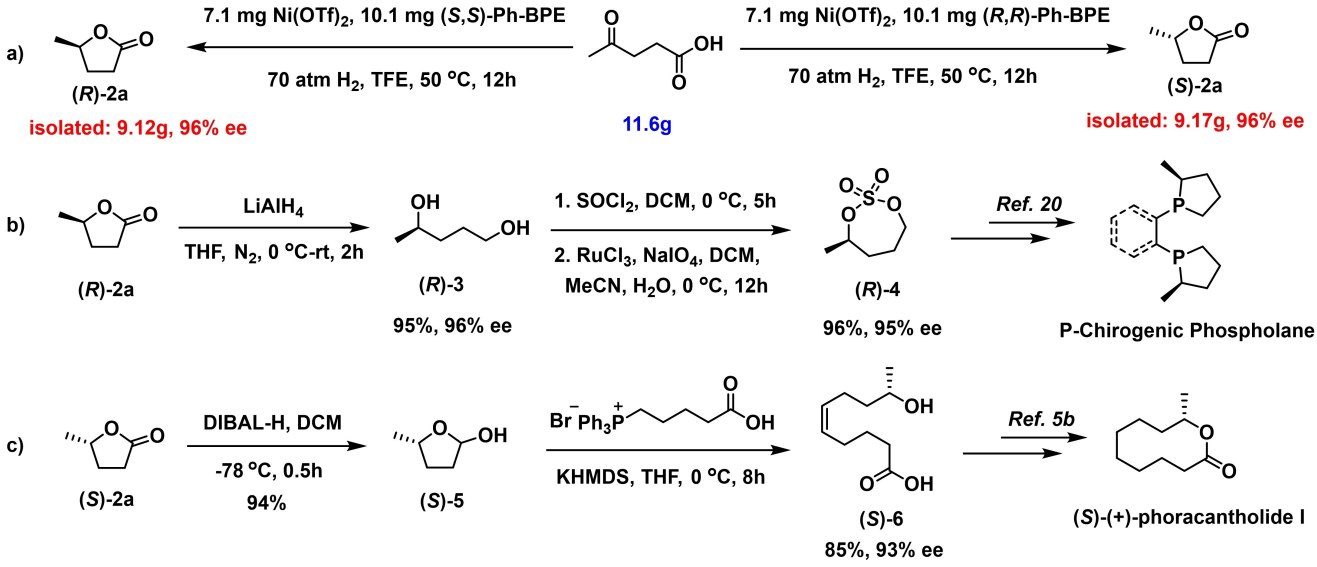

Scheme 9. The gram-scale preparation and transformation of chiral GVL.

catalytic system was demonstrated by the efficient hydrogenation of different aliphatic γ- and δ-ketoacids. Finally, levulinic acid from a real biomass feedstock could be also used for the production of chiral GVL without loss of ee value.

Author contributions

C.-Q. Deng: data curation, investigation, formal analysis, and writing original draft; J. Liu: DFT calculation. J.-H. Luo and L.-J. Gan: investigation. Y. Fu: resources and supervision; J. Deng: conceptualization, project administration, resources, supervision, and writing review and editing.

Acknowledgements

This work was supported by the National Key R&D Program of China (2018YFB1501604) and the National Natural Science Foundation of China (21875239). The authors thank the Hefei Leaf Biotech Co., Ltd and Anhui Kemi Machinery Technology Co., Ltd for free samples and equipment that benefited our ability to conduct this study.

Conflict of Interest

There are no conflicts to declare.

Data Availability Statement

The data that support the findings of this study are available in the Supporting Information of this article.

Keywords: Asymmetric Hydrogenation · Chiral Lactones · Homogeneous Catalysis · Levulinic Acid · Nickel

[1] a) J. C. Serrano-Ruiz, R. Luque, A. Sepúlveda-Escribano, *Chem. Soc. Rev.* **2011**, *40*, 5266–5281; b) W. Schutyser, T. Renders, S. Van den Bosch, S. F. Koelewijn, G. T. Beckham, B. F. Sels, *Chem. Soc. Rev.* **2018**, *47*, 852–908; c) W. Leitner, J. Klankermayer, S. Pichinger, H. Pitsch, K. Kohse Höinghaus, *Angew. Chem. Int. Ed.* **2017**, *56*, 5412–5452; *Angew. Chem.* **2017**, *129*, 5500–5544; d) S. Fu, Z. Shao, Y. Wang, Q. Liu, *J. Am. Chem. Soc.* **2017**, *139*, 11941–11948; e) J. Wu, L. Shen, S. Duan, Z. Chen, Q. Zheng, Y. Liu, Z. Sun, J. H. Clark, X. Xu, T. Tu, *Angew. Chem. Int. Ed.* **2020**, *59*, 13871–13878; *Angew. Chem.* **2020**, *132*, 13975–13982.

[2] a) F. M. A. Geilen, B. Engendahl, A. Harwardt, W. Marquardt, J. Klankermayer, W. Leitner, *Angew. Chem. Int. Ed.* **2010**, *49*, 5510–5514; *Angew. Chem.* **2010**, *122*, 5642–5646; b) F. M. A. Geilen, B. Engendahl, M. Holscher, J. Klankermayer, W. Leitner, *J. Am. Chem. Soc.* **2011**, *133*, 14349–14358; c) A. Phanopoulos, A. J. P. White, N. J. Long, P. W. Miller, *ACS Catal.* **2015**, *5*, 2500–2512; d) T. J. Korstanje, J. Ivar van der Vlugt, C. J. Elsevier, B. de Bruin, *Science* **2015**, *350*, 298–302.

[3] a) J. P. Lange, R. Price, P. M. Ayoub, J. Louis, L. Petrus, L. Clarke, H. Gosselink, *Angew. Chem. Int. Ed.* **2010**, *49*, 4479–4483; *Angew. Chem.* **2010**, *122*, 4581–4585; b) P. Sun, G. Gao, Z. Zhao, C. Xia, F. Li, *ACS Catal.* **2014**, *4*, 4136–4142; c) J. He, Z. Wu, Q. Gu, Y. Liu, S. Chu, S. Chen, Y. Zhang, B. Yang, T. Chen, A. Wang, B. M. Weckuysen, T. Zhang, W. Luo, *Angew. Chem. Int. Ed.* **2021**, *60*, 23713–23721; *Angew. Chem.* **2021**, *133*, 23906–23914.

[4] a) L. Deng, J. Li, D. M. Lai, Y. Fu, Q. X. Guo, *Angew. Chem. Int. Ed.* **2009**, *48*, 6529–6532; *Angew. Chem.* **2009**, *121*, 6651–6654; b) B. Zada, R. Zhu, B. Wang, J. Liu, J. Deng, Y. Fu, *Green Chem.* **2020**, *22*, 3427–3432; c) Q. Yuan, H. H. van de Bovenkamp, Z. Zhang, A. S. Piskun, S. Sami, R. W. A. Havenith, H. J. Heeres, P. J. Deuss, *ACS Catal.* **2021**, *11*, 10467–10477.

[5] a) P. Koh, T. Loh, *Green Chem.* **2015**, *17*, 3746–3750; b) R. Datrika, S. R. Kallam, S. R. Khobare, V. S. Gajare, M. Kommi Rama Mohan, H. S. Vidavalur, T. V. Pratap, *Tetrahedron: Asymmetry* **2016**, *27*, 603–607; c) E. L. Stangeland, T.

Sammakia, *J. Org. Chem.* **2004**, *69*, 2381–2385; d) K. Mori, *Tetrahedron* **1975**, *31*, 3011–3012; e) J. D. White, J. C. Amedio, *J. Org. Chem.* **1989**, *54*, 736–738.

[6] a) M. El Hadi, F. Zhang, F. Wu, C. Zhou, J. Tao, *Molecules* **2013**, *18*, 8200–8229; b) P. de Ferron, C. Thibon, S. Shinkaruk, P. Darriet, L. Allamy, A. Pons, *J. Agric. Food Chem.* **2020**, *68*, 13344–13352.

[7] a) J. M. Tukacs, B. Fridrich, G. Dibó, E. Székelya, L. T. Mika, *Green Chem.* **2015**, *17*, 5189–5195; b) M. L. Li, Y. Li, J. B. Pan, Y. H. Li, S. Song, S. F. Zhou, Q. L. Zhou, *ACS Catal.* **2020**, *10*, 10032–10039.

[8] a) P. V. Ramachandran, H. C. Brown, S. Pitre, *Org. Lett.* **2001**, *3*, 17–18.

[9] a) A. Díaz-Rodríguez, W. Borzęcka, I. Lavandera, Vi. Gotor, *ACS Catal.* **2014**, *4*, 386–393; b) T. Wang, X.-Y. Zhang, Y.-C. Zheng, Y.-P. Bai, *Chem. Commun.* **2021**, *57*, 10584–10587.

[10] a) C. S. Shultz, S. W. Krska, *Acc. Chem. Res.* **2007**, *40*, 1320–1326; b) P. Etayo, A. Vidal-Ferran, *Chem. Soc. Rev.* **2013**, *42*, 728–754; c) P. J. Chirik, *Acc. Chem. Res.* **2015**, *48*, 1687–1695; d) M. Shevlin, M. R. Friedfeld, H. Sheng, N. A. Pierson, J. M. Hoyt, L. Campeau, P. J. Chirik, *J. Am. Chem. Soc.* **2016**, *138*, 3562–3569; e) J. Liu, S. Krajangsri, J. Yang, J. Li, P. G. Andersson, *Nat. Catal.* **2018**, *1*, 438–443; f) M. R. Friedfeld, H. Zhong, R. T. Ruck, M. Shevlin, P. J. Chirik, *Science* **2018**, *360*, 888–893.

[11] a) T. Ohkuma, D. Ishii, H. Takeno, R. Noyori, *J. Am. Chem. Soc.* **2000**, *122*, 6510–6511; b) T. Ohkuma, C. A. Sandoval, R. Srinivasan, Q. Lin, Y. Wei, K. Muñiz, R. Noyori, *J. Am. Chem. Soc.* **2005**, *127*, 8288–8289; c) T. Touge, T. Hakamata, H. Nara, T. Kobayashi, N. Sayo, T. Saito, Y. Kayaki, T. Ikariya, *J. Am. Chem. Soc.* **2011**, *133*, 14960–14963; d) J. H. Xie, X. Y. Liu, X. H. Yang, J. B. Xie, L. X. Wang, Q. L. Zhou, *Angew. Chem. Int. Ed.* **2012**, *51*, 201–203; *Angew. Chem.* **2012**, *124*, 205–207; e) Q. Hu, Z. Zhang, Y. Liu, T. Imamoto, W. Zhang, *Angew. Chem. Int. Ed.* **2015**, *54*, 2260–2264; *Angew. Chem.* **2015**, *127*, 2288–2292; f) N. Arai, T. Namba, K. Kawaguchi, Y. Matsumoto, T. Ohkuma, *Angew. Chem. Int. Ed.* **2018**, *57*, 1386–1389; *Angew. Chem.* **2018**, *130*, 1400–1403; g) F. H. Zhang, F. G. Zhang, M. L. Li, J. H. Xie, Q. L. Zhou, *Nat. Catal.* **2020**, *3*, 621–627.

[12] For reviews, see: a) K. Gopalaiah, *Chem. Rev.* **2013**, *113*, 3248–3296; b) H. Pellissier, H. Clavier, *Chem. Rev.* **2014**, *114*, 2775–2823; c) Y.-Y. Li, S.-L. Yu, W.-Y. Shen, J.-X. Gao, *Acc. Chem. Res.* **2015**, *48*, 2587–2598; d) Z. Zhang, N. A. Butt, M. Zhou, D. Liu, W. Zhang, *Chin. J. Chem.* **2018**, *36*, 443–454; e) L. Alig, M. Fritz, S. Schneider, *Chem. Rev.* **2019**, *119*, 2681–2751; f) Y. Liu, X.-Q. Dong, X. Zhang, *Chin. J. Org. Chem.* **2020**, *40*, 1096–1104; g) F. Agbossou-Niedercorn, C. Michon, *Coord. Chem. Rev.* **2020**, *425*, 213523–213549; h) J. Wen, F. Wang, X. Zhang, *Chem. Soc. Rev.* **2021**, *50*, 3211–3237; i) H. Wang, J. Wen, X. Zhang, *Chem. Rev.* **2021**, *121*, 7530–7567.

[13] For recent examples, see: a) M. B. Widegren, G. J. Harkness, A. M. Z. Slawin, D. B. Cordes, M. L. Clarke, *Angew. Chem. Int. Ed.* **2017**, *56*, 5825–5828; *Angew. Chem.* **2017**, *129*, 5919–5922; b) M. Garbe, K. Junge, S. Walker, Z. Wei, H. Jiao, A. Spannenberg, S. Bachmann, M. Scalone, M. Beller, *Angew. Chem. Int. Ed.* **2017**, *56*, 11237–11241; *Angew. Chem.* **2017**, *129*, 11389–11393; c) L. Zhang, Y. Tang, Z. Han, K. Ding, *Angew. Chem. Int. Ed.* **2019**, *58*, 4973–4977; *Angew. Chem.* **2019**, *131*, 5027–5031; d) F. Ling, H. Hou, J. Chen, S. Nian, X. Yi, Z. Wang, D. Song, W. Zhong, *Org. Lett.* **2019**, *21*, 3937–3941; e) L. Zhang, Z. Wang, Z. Han, K. Ding, *Angew. Chem. Int. Ed.* **2020**, *59*, 15565–15569; *Angew. Chem.* **2020**, *132*, 15695–15699; f) L. Zeng, H. Yang, M. Zhao, J. Wen, J. H. R. Tucker, X. Zhang, *ACS Catal.* **2020**, *10*, 13794–13799.

[14] P. O. Lagaditis, P. E. Sues, J. F. Sonnenberg, K. Y. Wan, A. J. Lough, R. H. Morris, *J. Am. Chem. Soc.* **2014**, *136*, 1367–1380.

[15] a) A. Zirakzadeh, K. Kirchner, A. Roller, B. Stöger, M. Widhalm, R. H. Morris, *Organometallics* **2016**, *35*, 3781–3787; b) J. F. Sonnenberg, K. Y. Wan, P. E. Sues, R. H. Morris, *ACS Catal.* **2017**, *7*, 316–326; c) S. A. M. Smith, P. O. Lagaditis, A. Lüpke, A. J. Lough, R. H. Morris, *Chem. Eur. J.* **2017**, *23*, 7212–7216; d) R. Huber, A. Passera, A. Mezzetti, *Organometallics* **2018**, *37*, 396–405.

[16] a) W. Gao, H. Lv, T. Zhang, Y. Yang, L. Chung, Y.-D. Wu, X. Zhang, *Chem. Sci.* **2017**, *8*, 6419–6422; b) Y. Guan, Z. Han, X. Li, C. You, X. Tan, H. Lv, X. Zhang, *Chem. Sci.* **2019**, *10*, 252–256; c) Y. Liu, Z. Yi, X. Yang, H. Wang, C. Yin, M. Wang, X.-Q. Dong, X. Zhang, *ACS Catal.* **2020**, *10*, 11153–11161; d) Y. Liu, Z. Yi, X. Tan, X.-Q. Dong, X. Zhang, *iScience* **2019**, *19*, 63–73; e) B. Li, J. Chen, Z. Zhang, I. D. Gridnev, W. Zhang, *Angew. Chem. Int. Ed.* **2019**, *58*, 7329–7334; *Angew. Chem.* **2019**, *131*, 7407–7412; f) D. Liu, B. Li, J. Chen, I. D. Gridnev, D. Yan, W. Zhang, *Nat. Commun.* **2020**, *11*, 5935–5944; g) Y. Hu, J. Chen, B. Li, Z. Zhang, I. D. Gridnev, W. Zhang, *Angew. Chem. Int. Ed.* **2020**, *59*, 5371–5375; *Angew. Chem.* **2020**, *132*, 5409–5413; h) B. Li, D. Liu, Y. Hu, J. Chen, Z. Zhang, W. Zhang, *Eur. J. Org. Chem.* **2021**, 3421–3425; i) P. Yang, Y. Sun, K. Fu, L. Zhang, G. Yang, J. Yue, Y. Ma, J. Zhou, B. Tang, *Angew. Chem. Int. Ed.* **2022**, *61*, e202111778; *Angew. Chem.* **2022**, *134*, e202111778.

[17] a) Y. Hamada, Y. Koseki, T. Fujii, T. Maeda, T. Hibino, K. Makino, *Chem. Commun.* **2008**, 6206–6208; b) T. Hibino, K. Makino, T. Sugiyama, Y. Hamada, *ChemCatChem* **2009**, *1*, 237–240.

[18] L. Falivene, Z. Cao, A. Petta, L. Serra, A. Poater, R. Oliva, V. Scarano, L. Cavallo, *Nat. Chem.* **2019**, *11*, 872–879.

[19] a) X. L. Du, L. He, S. Zhao, Y. M. Liu, Y. Cao, H. Y. He, K. N. Fan, *Angew. Chem. Int. Ed.* **2011**, *50*, 7815–7819; *Angew. Chem.* **2011**, *123*, 7961–7965; b) J. M. Tukacs, M. Novák, G. Dibób, L. T. Mika, *Catal. Sci. Technol.* **2014**, *4*, 2908–2912.

[20] G. Hoge, *J. Am. Chem. Soc.* **2004**, *126*, 9920–9921.

Manuscript received: November 23, 2021
Accepted manuscript online: January 31, 2022
Version of record online: ■■, ■■

Research Articles

Homogeneous Catalysis

C.-Q. Deng, J. Liu, J.-H. Luo, L.-J. Gan, J. Deng,* Y. Fu* ——— **e202115983**

Proton-Promoted Nickel-Catalyzed Asymmetric Hydrogenation of Aliphatic Ketoacids

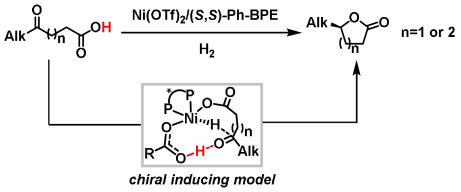

- *Earth-abundant metal catalyst*
- *Base-free and 20 examples*
- *High activity* (up to 7500 S/C)
- *Excellent enantioselectivity* (up to 99% ee)

A robust and efficient nickel–phosphine complex has been discovered for the asymmetric hydrogenation of aliphatic ketoacids. A proton promoted the activation of C=O bonds and controlled the stereoselectivity through hydrogen bonds to obtain the corresponding products in high yields with excellent enantioselectivities.